

# An application of a genetic algorithm based on Particle Swarm Optimization to a multiple responses problem arising in the Tube Hydroforming Process

Hamza A. GHULMAN, Mohammed YUNUS\*

Mechanical Engineering Department, College of Engineering and Islamic Architecture,  
Umm Al-Qura University, Abdiah, Makkah, Kingdom of Saudi Arabia  
haghulman@uqu.edu.sa, myhasan@uqu.sa

\*Corresponding author: Mohammed YUNUS  
myhasan@uqu.sa

**Abstract:** Tube Hydroforming (THF) is a relatively new manufacturing process mainly used in the automotive industry from the past decades, offering potential alternatives to lightweight materials. THF can significantly govern saving energy, offering several advantages over stamping and welding processes. Automotive sectors require complex-shaped extruded hollow tubes due to free-forming and calibration. THF requires less thinning to provide improved structural strength and stiffness. Lightweight vehicle units requiring less maintenance if THF are implemented with less formable Inconel 600 tubes. The impact of Hydroforming parameters (HFP) like P (internal pressure), L (axial movement), and F (tube length) on the tube output's quality like Bulging and Thinning ratios (BR&TR) are studied. RSM (Response surface methodology) was employed to develop empirical relations between HFP and experimental outputs. Particle Swarm Optimization (PSO) algorithm is applied to obtain a large amount of optimized data set for HFPs combination while simultaneously enhancing BR and reducing TR. Genetic algorithms improve the Pareto front optimized solutions of PSO's accuracy by prolonging convergence. Increasing P and L parameters values will significantly affect the output's quality. Proposed methods have performed outstanding (they avoided tube's local necking and failures like wrinkle and bursting) and the results were not possible with other techniques.

**Keywords:** Hydroforming, Bulge ratio, Thinning ratio, pareto optimal front, Swarm Optimization.

## 1. Introduction

Hydroforming came into existence from 1940 to 1950 to reduce manufacturing costs for the forming process of production compared to deep drawing components in small quantities (Davis, 1945). Later in 1990, an/ automotive field was increasingly attracted by the Hydroforming (HF) method, a forming process using highly pressurized water /fluids to bend each component either by tube or sheet hydroforming. A straight or pre-bent tube-shaped blank of required length held between the die, which is closed with necessary clapping force in tube HF. Subsequently, an axial force (AF) at the two ends of the tube is employed to bend the tube following the die shape using highly pressurized water mixed with emulsion/ liquid into the pipe by engaging with axial cylinders, the leakages of the liquid at both ends of the tube is prevented. High pressure exists inside the tube where its material starts yielding and takes on the die cavity shape such that the component is molded. Various experimentation and analytical investigations of bulge shaped tube HF assumed that the entire tube length under tension and corresponding results for free bulge were reported (Woo et al., 1973). The effect of lubricant and material (copper, brass, low carbon steel, and aluminum) on HF using the T-shaped die under the oil-pressurizing medium is studied. Results are shown as a function extrusion height accomplishable (Limb, Chakrabarty, Garber & Roberts, 1976 ).

The actual strain around necking using pre-strain value, strain-hardening exponential (SHE) value, and stress ratio was derived (Sauer, Gotera, Robb & Huang, 1978). Using experiments and thorough analysis of stresses and strains in case of anisotropy sheet metals by following "Hill's theory of plastic anisotropy" is explained (Woo & Woo, 1978). The impact of the SHE and material anisotropy property on components produced by bulge hydroforming is explained with the maximum pressure. It was applied inside the tube as a blank tubular diameter, thickness, SHE, and strength coefficient considering without AF examined (Chebbah et al., 2016; Rudraksha et al., 2017). Deforming ability and forming limits of thin-walled Al pipes were examined under the combined effect of internal pressure (IP) and AF regulated using a computer-based regulator to obtain a prespecified stress ratio (Manabe, Mori & Suzuki, 1984). The impact of material

properties (such as SHE, plasto-anisotropic, and surplus compression stress) on free bulge HF has been investigated (Fuchizawa et al., 1987; Manabe et al., 2002). The impact of IP and axial length on extrusion height and height of components on 'T' and X shaped Al alloy tube were examined (Fuchizawa, Narazaki & Yuki, 1993). The deformation of axisymmetric components and T-shaped parts by enlargement due to IP and strengthening by AF were studied (Dohmann & Hartl, 1996). The impact of various input factors of "Bulge Tube Hydroforming" (BTHF) was widely explained with the structured, logical models (Ahmed, & Hashmi, 1997). These models are employed to find the constraints of free THF, the effect of control variables on the loading path, and the deformation during their experimentation (Asnafi et al., 2020).

Many numerical simulation sequences and trials were conducted to investigate the tube forming ability (Manabe, Mori & Suzuki, 1984). A self-feeding procedure was suggested to reduce the explore for loading pathways to an appropriate reign of curves. They are only suitable for axisymmetric BTHF parts and not suitable for T and Y-shaped parts (Manabe & Amino, 2002). Optimal loading pathways via different optimization techniques like sensitivity analysis and response surface were suggested (Yang et al., 2001; Genlin et al., 2002). The "Finite Element" (FE) analysis using the sequence of simulations with commercial FE code was used to investigate the cold-HF of a T shape parts (like fluid elongation, AF, and the opposing force) for bursting mode. Comparatively, it is seen as a non-recoverable failure mode than buckling and wrinkling modes in the BTHF process (Rudraksha & Gawande, 2017). FE analysis of BTHF for evaluating explosion failure of ductile based fracture criterion using stress-strain results was briefed (Kim, Kang, & Kang, 2003). The explosion failure was predicted in BTHF, considering the plastic variability by adopting a rising theory of plasticity in anisotropic material and the HF. The stress regulating diagram was predicted from the scattered necking principle (Kim, Song, Kang & Kim, 2009). Optimization technique (HEEDS software) accompanying the FEA (LS-DYNA) was used for improving the forming factors in BTHF of high-strength steels. They maximize forming capability by evaluating an optimal set of characteristics like IP and AF (Abedrabbo et al., 2009). The inverse of FEA for anisotropic THF of T and Y shaped parts using classical EDIA of ABAQUS software was carried out [4]. FE simulations and experimental results of BTHF on finding the impact of factors shown a higher SHE. Selection of anisotropic substance for tube brings good forming capability and maintaining appropriate lubrication get the uniform wall thickness distribution (Asnafi et al., 2020).

From the literature, few gaps like the deformation behavior of superalloy Inconel 600 during THF have not yet been sufficiently clarified. Further research work demands to know whether forming capability and characteristics differ from changing the material. Proposed work includes investigation on the impact of HF input parameters (HFIP) such as IP, AF, and tube length on the output characteristics to maximize bulge and minimum thinning of the tube without necking failure in THF. Also, the aim is to determine the optimal set of factors simultaneously satisfying the conditions and forecasting the empirical form of models for the outputs of THF. It is observed that the standard modeling tools applied for the analysis of the THF as of today are the Taguchi technique, Grey Relational Analysis, "Artificial neural networks" ANN and other simulation tools like LS DYNA, Workbench, etc., (Yunus et al., 2016; Yunus et al., 2018; Yunus et al., 2019; Yunus et al., 2019; Yunus et al., 2020). These have certain limitations, such that they cannot find more than one quantitative relationship between the HFIP and the responses, the accurate selection and control of HFIP for optimum performance.

Hence, effective, efficient, and economical utilization of THF requires a precise modeling and optimization methodology. The literature review reveals that the PSO (Particle swarm optimization) is effective, inexpensive, and comparatively easy to use and yields accurate process models with a maximum HFIP combination to use as a reference manual. This method has been widely used for process modeling of several manufacturing processes. This method has not been applied for modeling tube hydroforming parameters of Inconel 600 tubes to the/our best knowledge. Besides, chosen responses, i.e., bulge ratio (BR), thinning ratio (TR), have been modeled and optimized for the first-time using Minitab statistical and MATLAB programming. From literature, the optimization methods used in earlier work were predominantly Taguchi based. Hence, in this work, a population-based algorithm called a genetic algorithm, and the Pareto front solution

method, multi objectives using PSO technique are used to optimize the chosen objective functions. The obtained solutions from optimization tool of MATLAB will be used as data sets for attaining maximum BR with minimum TR to utilize as reference manual in future satisfying various conditions of the process.

## 2. Materials and methodology

The 200-ton capacity THF machine has a controller for regulating IP and AF inputs automatically using computer programming under the different strain paths with die arrangement for the free bulge tests. A horizontally placed tube held between the two die portions and hydraulic ram is applied with a satisfactory clamping force in the free bulge test. After closing two half sections of dies properly, both axial punches were forwarded for closing both ends to protect the tube for applying the AF (maximum capacity of 40 tons) to feed extra material in the expansion region. The maximum F required is less than one-fourth of its capacity as higher than this leads to buckling or wrinkle effect of the tube. The water is filled in the tube using the punch's left side and then its movement back and forth to remove excess air and seal the tube again. The IP and AF are regulated, and bulge height of heat-treated Inconel 600 tubes having fixed diameter (57.15mm) and thickness (1.45mm) with varying lengths (195mm, 210mm, and 225mm) is measured using "Linear variable Differential Transducer" (LVDT).

Using "Programmable Logical Controller" (PLC) and emergency stop, the required loading path is regulated with the program provided to it. All the dimensions and Inconel 600 mechanical characteristics of the tube were delivered before running the free bulge test (refer to Figure 1) of THF. The aim is to attain maximum bulging defined by BR without any failure. The optimized input factors are achieved by developing the mathematical expressions for predicting the responses. The procedures suggested in the present investigation may be used to predict the empirical models. Further, these empirical models can be solved by using any evolutionary algorithms.

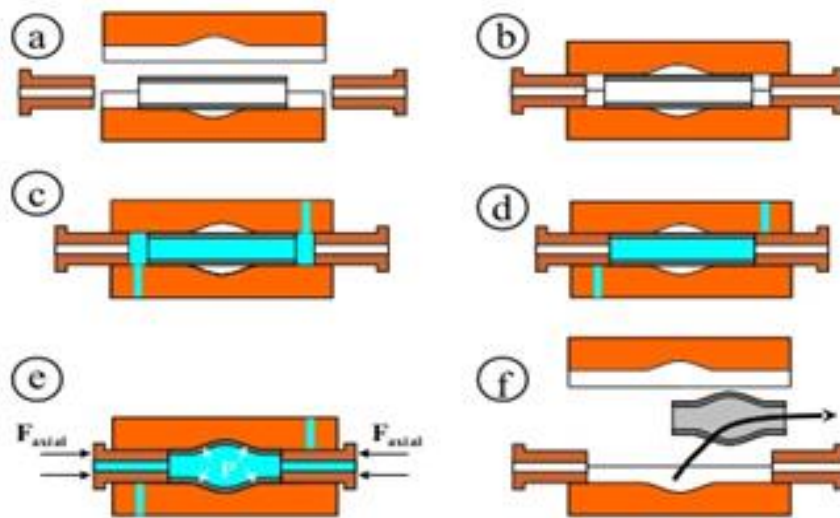


**Figure 1.** Tube hydroforming technique [9]

Several scholars worked for the advancement of the THF process to simplify the process and make suitable for forming. To decrease the number of trials for examining the impact of HFIP on the THF process for minimizing the cost is condensed as per Taguchi orthogonal array (OA) without upsetting the quality of the analysis because of its successful application in metal forming (Sokolowski et al., 2000; Yang et al., 2001).  $L_9$  OA is selected to study the conduction of tests on an annealed Inconel 600 tube and convert the trial results into mathematical equations by RSM (response surface methodology). MM's competence developed by RSM is inspected using ANOVA (analysis of variance) provided  $R^2$  (regression coefficient) value. Also, surface plots will be studied for the impact of HFIP on the maximization of BR and minimization of TR using Minitab digital

software. Two process responses namely, BR denoted by  $D_f/D_o$  ( $D_f$  and  $D_o$  are the final and original diameter at bulge point and TR represented by  $(T_i - T_f) / T_i$ , (where  $T_i$  and  $T_f$  are the original and final thickness at the highest bulging spot) are indicated in Figure 2.

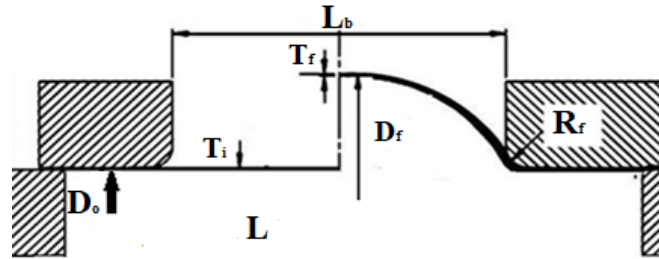


**Figure 2.** Free bulge Specifications of hydroforming technique (Sokolowski, Gerke, Ahmetoglu & Altan, 2000)

From the previous research and pilot experiments, it is noticed that the inside pressure ( $P$ ), axial movement ( $F$ ), and tube length ( $L$ ) are the most guiding factors affecting the maximum BR and minimum TR variation of the tube. Three HFIPs were selected, altering one each time; nine experiments were carried using the THF facility to find each HFIP's working levels as given in Table 1.

**Table 1.** Various levels of process variables

Input variables and Notations	Units	Levels		
		1	2	3
Internal Pressure ( $P$ )	Bar	225	250	275
Axial Movement ( $F$ )	mm/sec	0.2	0.35	0.5
Length of the Tube ( $L$ )	Mm	190	210	230

The responses maximum bulge after hydroforming, toolmakers microscope, and digital micrometer are used. The samples were then cut into two halves horizontally to measure the bulge and thickness after THF using above said instruments. For every response combination, the result is noted by an average of three values at three different locations of the maximum bulge point and recorded as listed in Table 2. The present research explores the impact of factors on the maximum bulge and minimum thickness variation.

**Table 2.**  $L_9$  Experimental observations as per Taguchi design

S.No.	Pressure ( $P$ )	Axial Force ( $F$ )	Tube Length ( $L$ )	$D_f$	$T_f$	$D_f/D_o$	$(T_i - T_f)/T_i$
1	225	0.20	190	82.87	1.291	1.45	0.11
2	225	0.35	210	62.87	1.25	1.10	0.14
3	225	0.50	230	68.58	0.97	1.20	0.33
4	250	0.20	210	88.59	1.26	1.55	0.13
5	250	0.35	230	57.72	1.09	1.01	0.25
6	250	0.50	190	69.72	1.10	1.22	0.24
7	275	0.20	230	85.72	1.25	1.50	0.14
8	275	0.35	190	86.87	1.28	1.52	0.12
9	275	0.5	210	66.3	1.00	1.16	0.31

## 2.1. GA based PSO technique for Multi-Response Optimization using MATLAB programming

On account of conflicting kinds of response qualities like BR and TR, the one set of optimized value of factors does not justify the objectives. To get many sets of optimized values for a combination of factors, under such a scenario, an evolutionary algorithm-based Multi-objective Optimization using Particle Swarm Optimization (MRPSO) provides improved performance when compared with the customary improvement strategies. Each data in the group has a flying velocity of  $V_{m(l)}$  into the demonstration space is characterized along with the position  $Y_{m(l)}$  vector. Several input variables articulate their constituents. Alterations of the data location use its previous position details and its current velocity (Walker et al., 2017). Thus,

$$V_{m(l+1)} = V_{m(l)} + c_1 \text{rand}_1 (P_{\text{bestm}} - Y_{m(l)}) + c_2 \text{rand}_2 (G_{\text{bestm}} - Y_{m(l)}) \quad (1)$$

$$Y_{m(l+1)} = Y_{m(l)} + V_{m(l+1)} \quad (2)$$

where  $Y_{m(l)}$  and  $V_{m(l)}$  are the current position and velocity at iteration  $h$ ;  $G_{\text{bestm}}$  and  $P_{\text{bestm}}$  "global and the personal best position of particle "m;  $c_1$ ,  $c_2$ , and  $\text{rand}$  " the cognition, social learning rate, and the random numbers varying between 0 to 1" respectively. To prevent a violent increase in velocity and the ambiguous random numbers instigated by the stochastic process of the 'search algorithm' in velocities updated in PSO, the Pareto front in combination with a genetic algorithm by conducting MRPSO will be used.

Multiple-response conditions provide an optimized group of HFIPs otherwise, optimizing individually, each response comprises conflicting solutions like one objective is improving by declining others in their final solution. The general and straightforward method is by establishing an absolute Pareto-front-solutions group or a graphic subgroup. The non-dominated (ND) are improved solutions obtained by reducing one or more responses, and by running an optimization of multi-output, a group of ND results will be obtained. A Pareto group is obtained by stabilizing the process within disagreeing responses. The projected work is to obtain an optimized combination set of HFIPs for maximum BR and minimum TR.

## 3. Results and discussion

### 3.1. Empirical modeling, adequacy tests like ANOVA and multiple $R^2$ for THF using RSM

The trial's output data from Table 2 are employed in Minitab statistical software (Yunus & Alsoufi, 2020), which computes the developed correlational model's (CM) regression coefficients. The polynomial fit conditions are detailed for the following Eqs (3) and (4)

$$BR = 8.8 - 0.0028 P + 2.14 F - 0.0682 L - 0.0625 P*F + 0.000149 P*L + 0.0605 F*L \quad (3)$$

$$TR = 3.56 - 0.0130 P - 1.93 F - 0.0174 L + 0.0011 P*F + 0.000063 P*L + 0.0110 F*L \quad (4)$$

ANOVA for the output responses BR & TR are specified in Tables 3 and 4, respectively, where generally models are considered vital if Probability >F but less than 0.05. BR and TR's ANOVA results (refer to Tables 3 and 4) show that the developed CMs are significant. Furthermore, to ensure the excellent agreement between developed models and the experiments, the multiple regression coefficients ( $R^2$ ); the CMs to total experimental variability ratio are used to check the fitness level (Fuchizawa, Narazaki & Yuki, 1993). In this work,  $R^2$  is very close to 1 indicates that the developed EMs are important and fit the experimental results. Referring to Tables 3, and 4,  $R^2=0.94$  (for BR) and 0.95 (for TR) represents that the EMs results fit experimental values up to 94%, and 0.95 respectively.

**Table 3.** ANOVA results of BR

Basis	Degree of Freedom	Adjusted SS	Adjusted MS	F-statistics Value	Probability Value
Model	6	0.055800	0.009300	4.89	0.179
Linear	3	0.045770	0.015257	8.03	0.113
P	1	0.000572	0.000572	0.30	0.638
F	1	0.025752	0.025752	13.55	0.067
L	1	0.005038	0.005038	2.65	0.245
2-Way Interaction	3	0.003700	0.001233	0.65	0.653
P*F	1	0.000021	0.000021	0.01	0.925
P*L	1	0.001152	0.001152	0.61	0.518
F*L	1	0.001260	0.001260	0.66	0.501
Error	2	0.003800	0.001900		
Total	8	0.059600			
	R <sup>2</sup>	97.62%	R <sup>2</sup> (adjusted)	94.50%	

Note: “Sum-of-Square (SS)” denotes the sum of squared differences from the average, and “Mean Square (MS)” value is computed by dividing a SS by the corresponding degrees of freedom.

The adjusted R<sup>2</sup> of BR (refer to Table 4) is 0.9582 is close to actual R<sup>2</sup> indicating that the developed model is adequate to handle variation. Similarly, TR satisfies the adequacy conditions as detailed in Table 4.

**Table 4.** TR from ANOVA results

Basis	Degree of Freedom	Adjusted		F-statistics Value	Probability Value
		SS	MS		
Model	6	0.296819	0.049470	2.70	0.295
Linear	3	0.277389	0.092463	5.04	0.170
P	1	0.069215	0.069215	3.78	0.191
F	1	0.035438	0.035438	1.93	0.299
L	1	0.102021	0.102021	5.56	0.142
2-Way Interaction	3	0.086536	0.028845	1.57	0.411
P*F	1	0.064038	0.064038	3.49	0.203
P*L	1	0.006438	0.006438	0.35	0.614
F*L	1	0.038402	0.038402	2.09	0.285
Error	2	0.036670	0.018335		
Total	8	0.333489			
	R <sup>2</sup>	95.00%	R <sup>2</sup> (adjusted)	93.02%	

Also, these CMs are tested for competence utilizing NPD (normal probability distribution) of residuals. Thus, the NPD of residuals of both outputs show all detailed data distribution is nearer line means adequacy is very much acceptable (Mohanty, Mahapatra & Singh, 2016). In both outputs (BR, TR), the distribution of data values is seen very near to or on the line of plots shown in Figure 3 (a) and 3 (b), signifying that the distribution of the errors is normal.

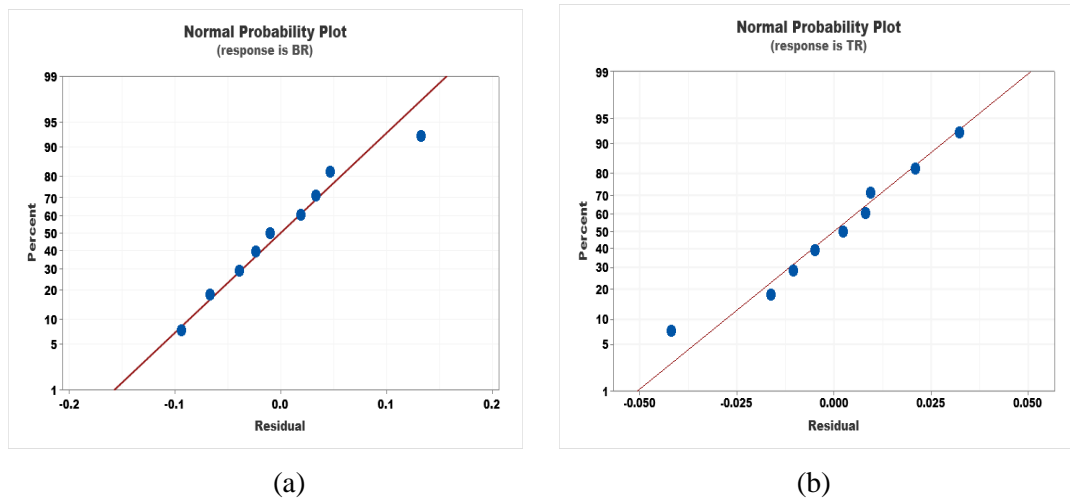


Figure 3. Normal probability distribution of residuals for (a) BR (b) TR

### 3.2. Confirmation experiments

The empirical equations of RSM are validated with the trial results using the combinations of HFIPs for BR and TR if deviation lies within limits. Percentage deviation is found by comparing the predicted and actual trial results presented in Table 5 by the ratio of the difference between trial and expected to the expected value. Deviation shows a perfect acceptance limit for the adopted methodology.

Table 5. Validation of results for BR and TR

No.	Process parameters			Bulge ratio			Thinning ratio		
	P in Bar	F in Mm/sec	L in mm	Predicted	Experiment	Deviation (%)	Predicted	Experiment	Deviation (%)
1	225	0.20	190	1.49625	1.45	3.09	0.10375	0.11	0.431
2	225	0.35	210	1.162125	1.10	5.35	0.177375	0.14	3.398
3	225	0.50	230	1.191	1.20	0.76	0.317	0.33	1.083
4	250	0.20	210	1.4445	1.55	7.30	0.0945	0.13	2.290
5	250	0.35	230	1.132	1.01	10.8	0.23675	0.25	1.312
6	250	0.50	190	1.2245	1.22	0.37	0.214	0.24	2.131
7	275	0.20	230	1.54175	1.50	2.71	0.14825	0.14	0.55
8	275	0.35	190	1.613875	1.52	5.82	0.132625	0.12	0.831
9	275	0.5	210	1.1415	1.16	1.621	0.3105	0.31	0.043

### 3.3. Impact of single and joint levels of HFIPs on BR

The influence of single HFIPs levels of IP shows a direct impact on BR variation like it increments with an increase of IP and yields to the higher load on the tube sheet. Because of

growing IP, the material keeps deforming until it reaches the ultimate strength. The impact of single HFIP levels of F also shows the same effect on BR like P. As this F was increasing, its value brought the material into an expansion state. Further material gets added to regulate and minimize the tube size (thickness) at the maximum bulging point. It provides necessary material at the expansion zone to attain the maximum bulging in this way.

Similarly, the influence of a third HFIP, L, on BR shows an inverse relationship as BR decreases with increasing L because an excess substance is not provided to a forming region by an AF. With the IP, the material gets thin at the maximum bulge point, and the tube will be under bursting failure, as exhibited in Figure 4a. Figure 4b elucidates the increasing level of AF and IP has a direct interactive influence on increasing BR. Due to the simultaneous increase of AF and IP, the BR rises more than AF and IP's individual impact. Figure 4c illustrates the interactive influence of L and IP on BR wherein BR increases with factor IP and decreasing with factor L. Joint impact of L and IP on BR shows it increased reasonably with the rise of both factors L and IP. Similarly, this is also true in the combined impact of HFIPs like L and AF, where BR increased moderately with the increase of both L and AF. At their individual levels, the BR value rises with the decrease of L and an increase of AF (refer to Figure 4d).

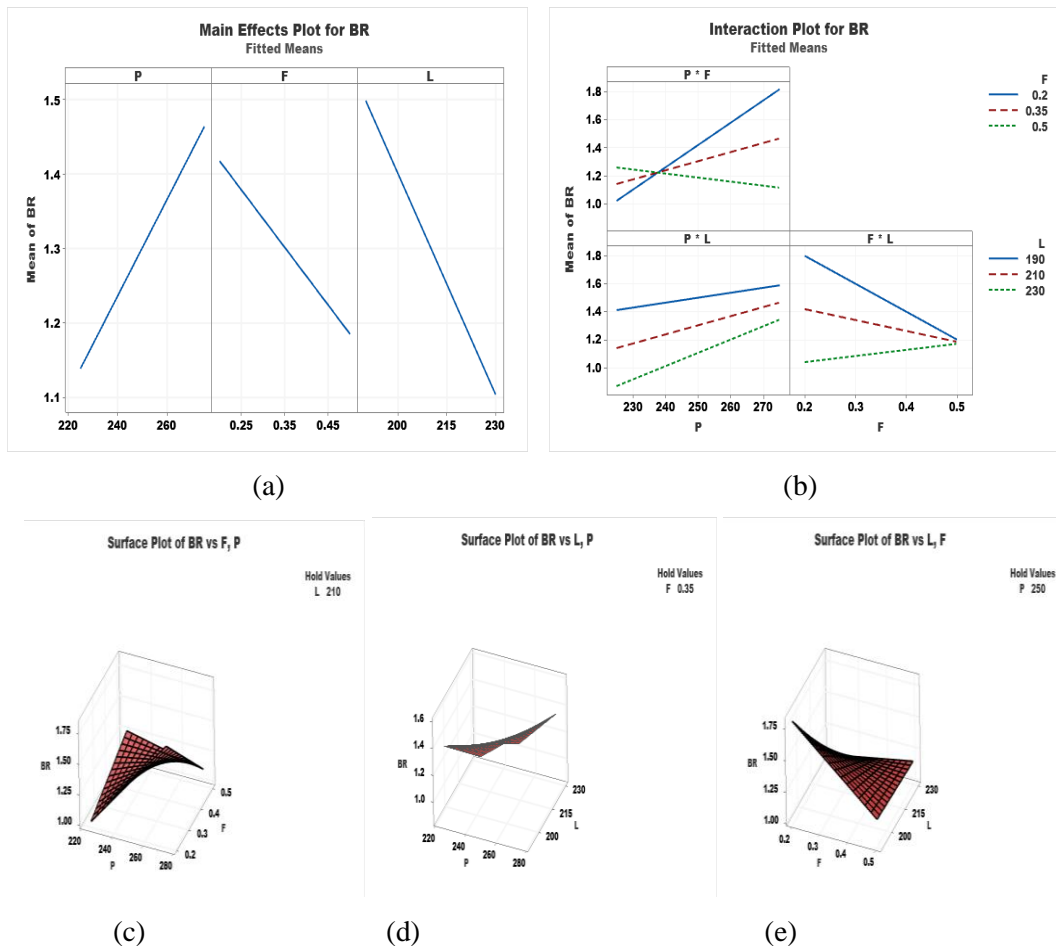
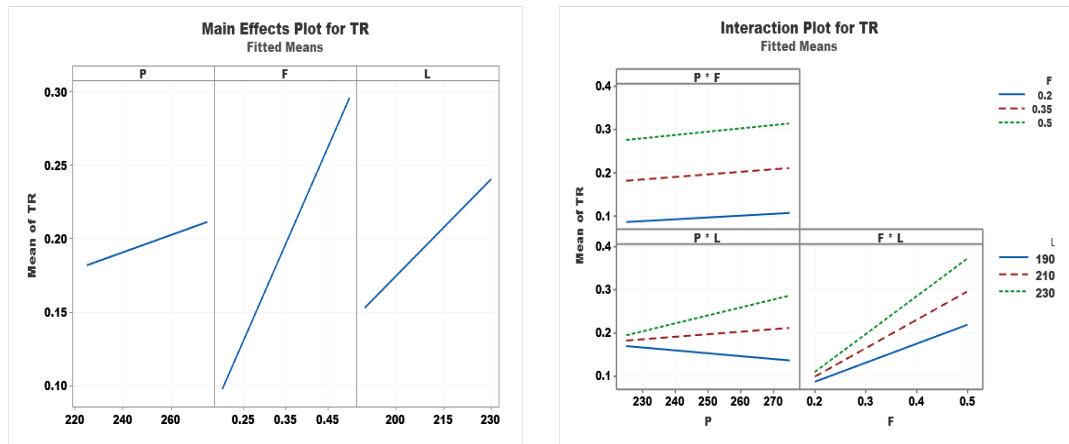


**Figure 4.** Main effect of (a) IP, AF, & L and Interaction effect of (b) of all factors (c) AF & IP (d) L & IP and (e) L & AF on BR

### 3.4. Single and joint level impact of HFIPs on TR

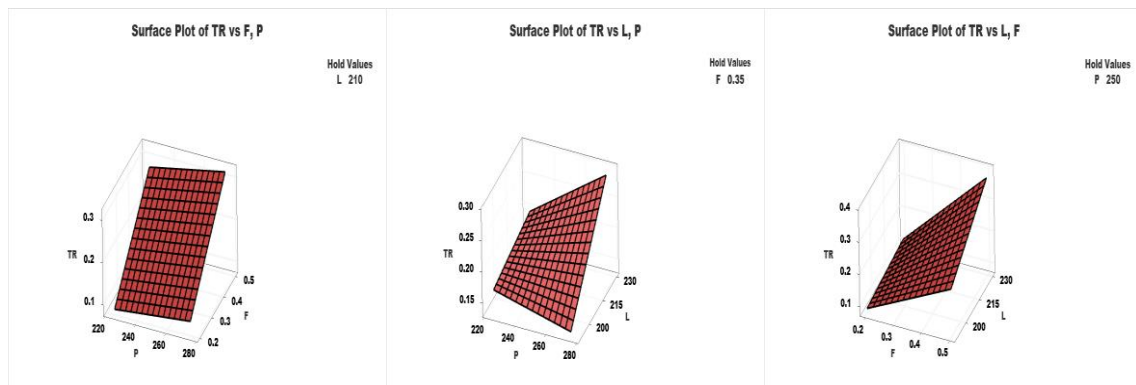
The importance of IP, AF, and L on TR are illustrated in Figure 5(a), show that the rise of TR occurs when IP increases as it causes the maximum bulge by thinning the tube. The TR is the ratio of difference of tube thickness to initial thickness. Therefore, a higher TR means additional variation in the thickness of the THF process. Similarly, the AF on TR shows that TR decreased

with the AF increase as it causes extra material to be drawn into the expansion zone. Also, it compensates for the thinning of the tube along with increased bulge of the tube. This produces the wrinkles on the final shape of the tube. L's impact on the increasing TR is growing as the required material does not reach the forming zone by the AF alone. With the increasing L, the higher AF is expected to drive the substance into the forming region.



(a)

(b)



(c)

(d)

(e)

**Figure 5.** Main effect of (a) IP, AF, & L and Interaction effect of (b) of all factors (c) AF & IP (d) & IP and (e) L & AF on TR

The Impact of factors increased TR with individual level of rising of IP and fall of AF. But at their combined level, TR has been increased satisfactorily with increasing AF and IP, as displayed in Figure 5b. Figure 5c demonstrates the TR increased with increasing combined levels of L and IP significantly. Referring to Figure 5 (d), TR rises with L's rising and AF's decreasing values when the individual HFIP levels are considered. The combined impact of L and AF showed that their increasing levels raise the TR relatively.

### 3.5. Interpretation of optimized state using GA based PSO

In this investigation, minimizing the TR and the maximization of BR were considered as the objective functions. Maximum BR/ bulging capacity signifies the tube material's distortion ability to bear out any shape by the THF process. On the other hand, the tube thickness was found to decrease with the increase of the bulging height, causing lower strength of the HF components. The objective functions for the BR and TR are formulated as optimizing model is given as shown in Figure 6 and Eqs (5) & (6) ( Mohanty, Mahapatra & Singh, 2016):

$$F(1) = (8.8 - 0.0028 * P + 2.14 * F - 0.0682 * L - 0.0625 * P * F + 0.000149 * P * L + 0.0605 * F * L); \quad (5)$$

$$F(2) = (-3.56 - 0.0130 * P - 1.93 * F - 0.0174 * L + 0.0011 * P * F + 0.000063 * P * L + 0.0110 * F * L); \quad (6)$$

The BR, TR, and the possible ranges of the input factors are identified with an outlook to have maximum BR and minimum TR without wrinkles or defects. Possible limits of the input factors are enlisted in Table 6.

**Table 6.** Permissible bounds of the input factors

Factors	Lower bound	Upper bound
Internal Pressure (P)	225	275
Axial Movement (AM)	0.2	0.5
Tube Length (L)	190	230

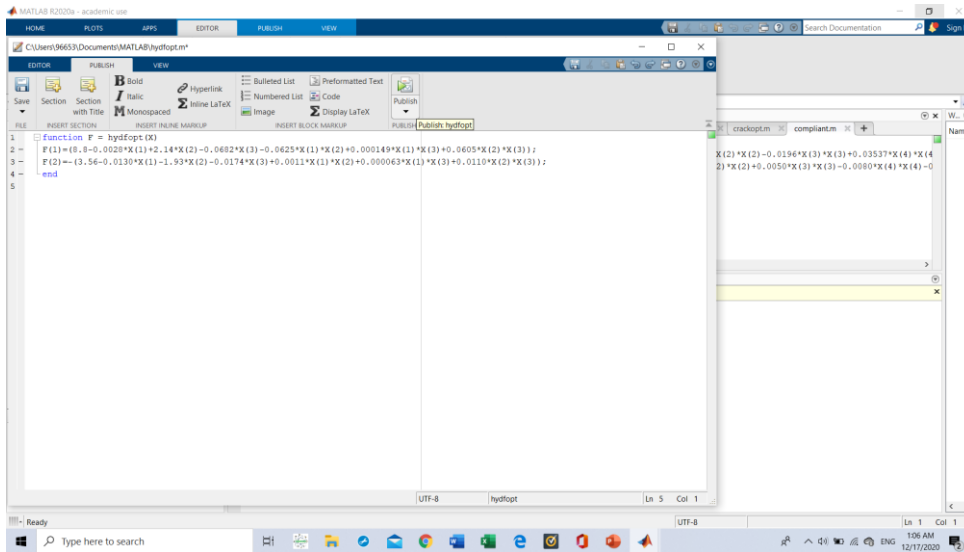


**Figure 6.** Objective functions defined in MATLAB workspace

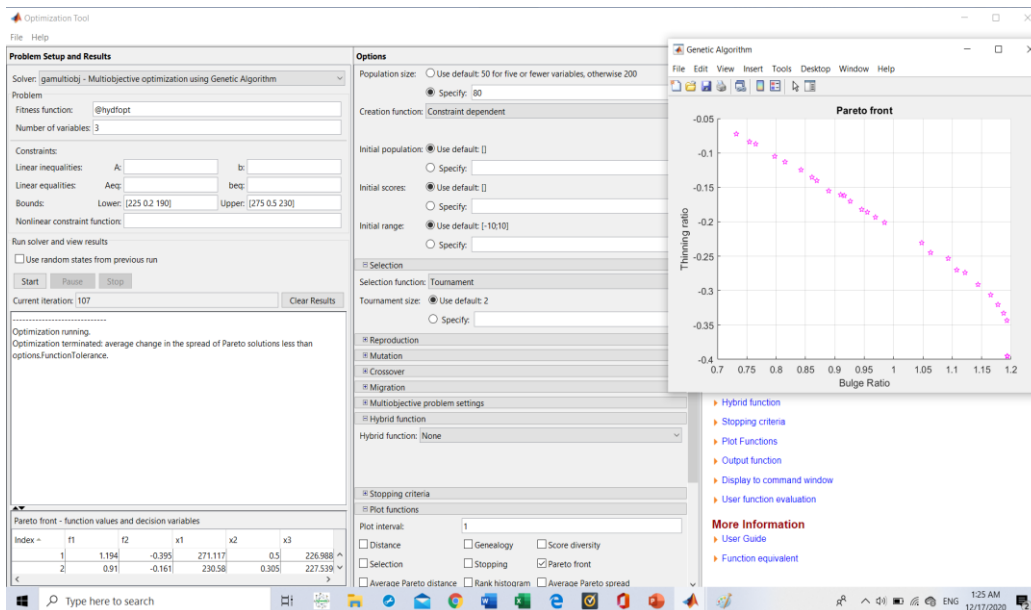


**Figure 7.** Optimization tool with limits, population size, pareto front plots etc.

After formulating the optimization state, the optimization problem is worked out using the genetic algorithm-based PSO for multiple objectives optimization using the MATLAB software optimization tool (refer Figure 7). Various sets of an optimal combination of HFIPs are

accomplished. An initial population of 80 is selected for evaluating objective functions, and it uses the Pareto front plot for the best global optimal solutions obtained, as shown in Figure 8. Corresponding values of plots are enlisted in Table 7.

**Table 7.** Best Global optimal solutions from PSO

S.No.	P	F	L	BR	TR
1	225.5	0.206	229.5	0.62453	0.068779
2	260.43	0.5	229.5	1.19837	0.3870145
3	241.53	0.463	229.49	1.16154	0.317444
4	226.73	0.3713	229.541	0.954252	0.210734
5	226.726	0.3589	229.538	0.93130	0.200273
6	225.412	0.233	229.604	0.67433	0.091798
7	227.237	0.3604	229.559	0.93840	0.20253
8	245.218	0.4825	229.513	1.1839	0.3414
9	226.242	0.307	229.538	0.82873	0.1555
10	254.698	0.4952	229.488	1.19702	0.37123
11	226.722	0.2732	229.596	0.7712	0.12795
12	227.762	0.4252	229.512	1.0596	0.25818
13	225.883	0.2559	229.576	0.7264	0.11183
14	231.986	0.4321	229.5	1.0907	0.27222
15	226.527	0.2079	229.518	0.6478	0.07249
16	226.181	0.3	229.572	0.8144	0.14953
17	232.647	0.4643	229.526	1.1412	0.30092
18	239.6598	0.4364	229.484	1.1289	0.2907
19	226.608	0.3206	229.55	0.8588	0.16775
20	244.414	0.4799	229.489	1.181	0.3375
21	227.649	0.4112	229.523	1.0338	0.2462
22	225.237	0.2001	229.629	0.6062	0.0636
23	252.539	0.4794	229.534	1.1922	0.3533
24	227.6	0.394	229.586	1.002	0.2317
25	229.03	0.3785	229.539	0.9855	0.22114
26	233.591	0.4423	229.516	1.1122	0.2841
27	226.434	0.3313	229.515	0.8774	0.17647
28	226.7197	0.3525	229.493	0.92	0.19485
29	230.209	0.3818	229.537	1.0001	0.2262

30	227.027	0.282	229.517	0.7931	0.13589
31	226.41	0.234	229.562	0.6937	0.09428
32	226.978	0.2367	229.544	0.7085	0.09754
33	225.779	0.2695	229.62	0.75	0.1231
34	225.478	0.2232	229.57	0.6568	0.08354
35	225.722	0.3165	229.55	0.8408	0.1627

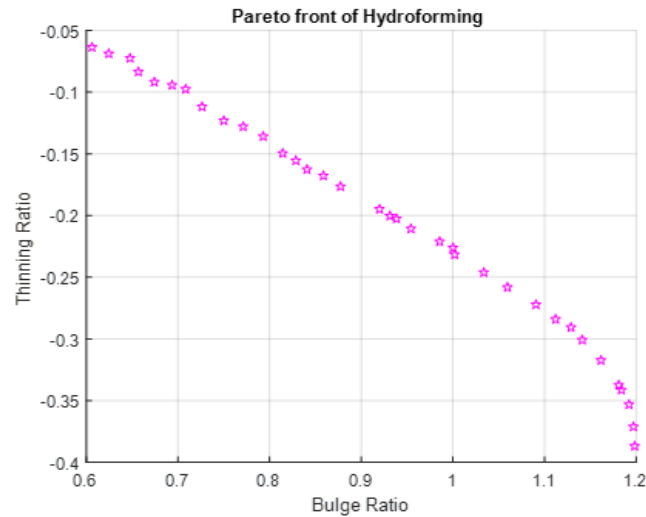


**Figure 8.** Pareto front solutions of GA based PSO of Multi outputs

## 4. Conclusions

In the present work, design of experiments-based trials, ANOVA for regression models, RS analysis, and GA based multi response PSO (using Pareto front solutions) were used to optimize the bulge and Thinning ratio. Impact of HFIPs, namely, IP, AF, and L for the THF of Inconel 600. Experiments were carried out as per the Taguchi OA table to bring down the attempts of experimentations significantly. RSM developed higher-order correlational models (CM) for the BR and TR as a function of chosen HFIPs. The predicted CM are tested for their significance using ANOVA,  $R^2$ , Rs plots, and the verification tests. The entire process is optimized using GA based MRPSO is automated with the recommended procedure. It yields optimal sets of combinations of HFIPs to help the machinists choose the right HFIPs according to process requirements.

These are the following observations derived from the present examinations.

1. From the simulation results, the  $R^2$  values of the second-order model obtained for bulge ratio and thinning ratio are found to be 0.9229, and 0.9611 shows a good fit of the predictive model results and the simulated results.
2. An optimizing state is subsequently framed to maximize the BR subjected to minimum TR as constraints. GA-based MRPSO with Pareto front plots is used to reach near the optimal global solution providing various combinations of an optimal set of parameters and satisfying the requirements.
3. The CM has been derived to predict the bulge ratio and thinning ratio for different combinations of factor settings from the RSM and validated with the experimental results to obtain high-quality parts of THF.

4. From the simulated results, it is observed that the increase in IP has a significant effect on the maximum BR and the effect of axial movement on TR has substantial influence are validated with experiments.
5. A bulge ratio of 1.4497 and thinning ratio of 0.1095 from experimental values and bulge ratio is increased to 1.464, and the thinning ratio is decreased to 0.106 after GA-MRPSO. It is noted at IP=268 Bar, AF=0.38 mm/sec, and L=198 mm are validated through test runs on the same experimental setup.
6. The interactive or combined effects of HFIPs like IP, AF, and L on the BR and TR are demonstrated and analyzed, showed that the combined impact of AF and IP is more on the enhancement of BR with lowering TR.

The present work was limited to a few HFIPs for conducting experiments and further analysis by increasing them to 4 or 5 depending on availability and THF machine's capacity. Furthermore, applying other available optimization techniques may also find the optimal HFIPs like ANN (Artificial neural networks), GA, etc. Comparisons were made between the two optimization techniques for suggesting the most suitable method. The present research is applied only for the free-forming stage and can be extended to analyze the calibration stage.

## REFERENCES

1. Abedrabbo, N. (2009). *Optimization methods for the tube hydroforming process applied to advanced high strength steels with experimental verification*. Journal of Materials Processing Technology, 209, 110-123.
2. Ahmed, M. & Hashmi, M. S. J. (1997). *Estimation of machine parameters for hydraulic bulge forming of tubular components*. Journal of Material Processing Technology, 64(1-3), 9-23. doi: 10.1016/S0924-0136(96)02549-6.
3. Asnafi, N. (2020). *Analytical modelling of tube hydroforming*. Thin-Walled Structures, 34(4), 295-330. 1999, Accessed: Aug. 08, 2020. [Online]. Available: [https://www.academia.edu/7516790/Analytical\\_modelling\\_of\\_tube\\_hydroforming](https://www.academia.edu/7516790/Analytical_modelling_of_tube_hydroforming).
4. Chebbah, M.-S. Hebbir, N. Kanit, T. & Dehimi, S. (2016). *Application of the Inverse Finite Element Approach for the Fast Simulation of Tube Hydroforming*. Journal of Procedia Technology, 22, 78-85. doi: 10.1016/j.protcy.2016.01.013.
5. Davis, E. A. (1945). *Yield and fracture of medium-carbon steel under combined stress*. Journal of Applied Mechanics, A13-A24.
6. Dohmann, F. & Hartl, C. (1996). *Hydroforming - A method to manufacture light-weight parts*. Journal of Material Processing Technology, 60(1-4), 669-676. doi: 10.1016/0924-0136(96)02403-X.
7. Fuchizawa, S. (1987). *Influence of Plastic Anisotropy on Deformation of Thin-walled Tubes in Bulge Forming*. Advanced Technology of Plasticity, 2, 727-732.
8. Fuchizawa, S., Narazaki, M. & Yuki, H. (1993). *Bulge Test for Determining Stress-Strain Characteristics of Thin Tubes*. Beijing, International Academic Publishers.
9. Genlin, J. C. & Labergere, C. (2002). *Numerical control strategies for the hydroforming of thin walled metallic tubes*. In Proceedings of International Conference and Workshop on

- Numerical Simulation of 3D Sheet Metal Forming Processes, (NUMISHEET ), 30(7), 499–504. doi: 10.1002/adfm.201909537.
10. Hydro forming. <https://www.slideshare.net/MehulPatel39/hydro-forming-27456214> (accessed Aug. 09, 2020).
  11. Kim, J., Kang, S. J. & Kang, B. S. (2003). *A prediction of bursting failure in tube hydroforming processes based on ductile fracture criterion*. International Journal of Advanced Manufacturing Technology, 22(5–6), 357–362. doi: 10.1007/s00170-002-1489-6.
  12. Kim, S. W., Song, W. J., Kang, B. S. & Kim, J. (2009). *Bursting failure prediction in tube hydroforming using FLS*. International Journal of Advanced Manufacturing Technology, 41(3–4), 311–322. doi: 10.1007/s00170-008-1488-3.
  13. Kwan C. T. & Lin, F. C. (2002). *Investigation of T-shape tube hydroforming with finite element method*. International Journal of Advanced Manufacturing Technology, 21(6), 420–425. doi: 10.1007/s001700300049.
  14. Limb, M. E., Chakrabarty, J., Garber, S. & Roberts, W. T. (1976). *Hydraulic forming of tubes*. Sheet Metal Industries, 676489(10), 418–424.
  15. Manabe, H. N. K. Mori, S. & Suzuki, K. (1984). *Bulge Forming of Thin Walled Tubes by Micro-Computer Controlled Hydraulic Press*. In Proceedings of 1<sup>st</sup> International Centre for Theoretical Physics (ICTP), 279–284.
  16. Manabe, K-I. & Amino, M. (2002). *Effects of process parameters and material properties on deformation process in tube hydroforming*. Journal of Material Processing Technology, 123, 285–291, doi: 10.1016/S0924-0136(02)00787-2.
  17. Mohanty, C. P., Mahapatra, S. S. & Singh, M. R. (2016). *A particle swarm approach for multi-objective optimization of electrical discharge machining process*. Journal of Intelligent Manufacturing, 27(6), 1171-1190.
  18. Oreijah, M. M. & Yunus, M. (2019). *A parametric analysis to evaluate the performance metrics of power generation system involving Trilateral Flash Cycle using three different working fluids for low grade waste heat*. AIMS Energy, 7(4), 483-492. doi: 10.3934/energy.2019.4.483.
  19. Rudraksha, S. P. & Gawande, S. H. (2017). *Optimization of Process Parameters to Study the Influence of the Friction in Tube Hydroforming*. Journal of Bio- and Tribo-Corrosion. 3(4), 56. doi: 10.1007/s40735-017-0117-9.
  20. Sauer, W. J., Gotera, A., Robb, F. & Huang, P. (1978). *Free Forming of Tubes under Internal Pressure and Axial Compression*. In Proceedings of the 6<sup>th</sup> North American Manufacturing Research Conference SME, Michigan (NAMRC-VI), 228-235.
  21. Sokolowski, T. K., Gerke, M., Ahmetoglu & Altan, T. (2000). *Evaluation of tube formability and material characteristics: hydraulic bulge testing of tubes*. Journal of Material Processing Technology, 98(1), 34–40.
  22. Sreenivasulu, B. & Prasanthi, G. (2017). *Empirical modeling & Analysis of Tube Hydroforming process of Inconel 600 using Response Surface Methodology*. International Journal of Mechanical & Mechatronics Engineering IJMME-IJENS, 17(01), 127-133.
  23. Strano, M., Jirathearanat, S., Shr, S. G. & Altan, T. (2004). *Virtual process development in tube hydroforming*. Journal of Material Processing Technology, 146(1), 130–136. doi: 10.1016/S0924-0136(03)00853-7.
  24. Walker, B. (2017). *Particle swarm optimization (PSO): advances in research and applications*. Nova Science Publishers.
  25. Woo, D. M. (1973). *Tube-bulging under internal pressure and axial force*. Journal of Engineering Material Technology Transactions, ASME, 95(4), 219–223. doi: 10.1115/1.3443156.

26. Woo D. & Woo, D. M. (1978). *Development of a bulge forming process*. Sheet Metal Industries, 55(5), 623–625.
27. Yang, J.-B., Jeon, B.-H. & Oh, S.-I. (2001). *Design sensitivity analysis and optimization of the hydroforming process*. Journal of Material Processing Technology, 113, 666–672.
28. Yunus, M. & Alsoufi, M. S. (2016). *Multi-output optimization of tribological characteristics control factors of thermally sprayed industrial ceramic coatings using hybrid Taguchi-grey relation analysis*. Friction, 4(3), 208–216. doi: 10.1007/s40544-016-0118-6.
29. Yunus, M. & Alsoufi, M. S. (2018). *Mathematical Modelling of a Friction Stir Welding Process to Predict the Joint Strength of Two Dissimilar Aluminium Alloys Using Experimental Data and Genetic Programming*. Modelling and Simulation in Engineering, 2018, Article ID 4183816, 18 pages. doi: 10.1155/2018/4183816.
30. Yunus, M. & Alsoufi, M. S. (2019). *Development of a heat pipe and grey based taguchi method for multi-output optimization to improve thermal performance using hybrid nanofluids*. Frontiers of Heat and Mass Transfer, 12 (11), 1-8. doi: 10.5098/hmt.12.11.
31. Yunus, M. & Alsoufi, M. S. (2019). *Mathematical Modeling of Multiple Quality Characteristics of a Laser Microdrilling Process Used in Al7075/SiCp Metal Matrix Composite using Genetic Programming*. Modelling and Simulation in Engineering, 2019. Article ID 1024365, 15 pages, doi: 10.1155/2019/1024365.
32. Yunus M. & Alsoufi, M. S. (2020). *Application of response surface methodology for the optimization of the control factors of abrasive flow machining of multiple holes in zinc and Al/SiCp MMC wires*. Journal of Engineering Science and Technology, 15(1), 655-674.



**Hamza A. GHULMAN** is an associate professor at the Department of Mechanical Engineering, College of Engineering and Islamic Architecture, Umm Al-Qura University, Makkah, Kingdom of Saudi Arabia. He majored in Mechanical Engineering Manufacturing from Ohio University, USA. He held positions of Head of the Mechanical Engineering Department, Vice Dean for Academic Affairs, Dean of the Custodian of the Two Holy Mosques institute of Hajj and Umrah Studies, and Dean for the college of Engineering and Islamic Architecture from 2001 to 2018. He was also Chair of the Technical, Advisory and the National Committee for the Saudi Building Code and Head of the technical team supervising the project designs to increase the capacity of the terminal in the Holy Mosque of Makkah. The college obtained the ABET international academic accreditation for two phases. He has published more than 80 research papers and books that have been printed in scientific journals, conferences, seminars and workshops in which he participated locally and internationally. He is a member in various national and international associations such as the Saudi Council of Engineers (adviser), the American Society of Engineers and Mechanics, the American Society of Engineers, the American Society of Industrial Engineers, the Scientific Society in Physical, the Arab Institute for Operation and many other societies.



**Mohammed YUNUS** is an Associate Professor (since 2014) in the Department of Mechanical Engineering, College of Engineering and Islamic Architecture, Makkah, Kingdom of Saudi Arabia. He graduated from the Faculty of Mechanical Engineering, Gulbarga University, India (1997), and has a master's degree in Machine design – Visvesvaraya Technological University, India (2000) and he also holds a Ph.D. Doctoral degree in Manufacturing, Thermal and Design - Anna University, Chennai, India (2012). The main areas of interest for the research activity include: Thermal Barrier Coatings, Composites, CAE, CFD, HVAC, Smart materials, CIM, Aerospace Components, Surface Characterization, Solid Mechanics, Fluid Mechanics, Optimization and Genetic Algorithm, renewable energy sources, water treatment, Compliant Mechanisms etc. He served as Post Graduation head and Under graduate head from 2008 to 2012. He has published more than 100 technical papers in reputed international, national journals and conferences. He has one United state patent.